*Journal of Applied Fluid Mechanics*, Vol. 12, No. 2, pp. 587-594, 2019.
Available online at www.jafmonline.net, ISSN 1735-3645, EISSN 1735-3645.
DOI: 10.29252/jafm.12.02.28914

# Inertia Effects in Rheodynamic Lubrication of an Externally Pressurized Converging Thrust Bearing using Bingham Fluids

G. Alexander Raymand† and I. Jayakaran Amalraj

*Department of Mathematics, SSN College of Engineering, Kalavakkam, Chennai, 603110, India.*

† *Corresponding Author Email: alexanderraymand@gmail.com*

(Received February 22, 2018; accepted September 4, 2018)

## ABSTRACT

Thrust bearing are innately developed to withstand axial load. When the bearing is subjected to high speed operations, heavy load, high stiffness etc., suggesting a change in the design of the bearing plays a vital role in its performance. Friction is developed between the circular plates while the bearing operates. To reduce this friction, the bearing is lubricated with lubricants such as mineral oil, greases etc., Generally, lubricants are classified into two types that is Newtonian and non-Newtonian. However, non-Newtonian fluids characterized by an yield value such as Bingham, Casson and Herschel Bulkley, are attracting the tribologists, at present. And also, the study of fluid inertia on thrust bearing is required to optimize the performance of the bearings. In this investigation, we have ventured to analyze the performance of the bearing by considering the combined effects of fluid inertia forces and non-Newtonian characteristic with Bingham fluid as lubricant in an externally pressurized converging circular thrust bearing. Such studies will be useful in the design of the bearing for the optimum performance using the appropriate lubricant in various machineries operating in an extreme condition in the industries. Averaging the inertia terms over film thickness and defining a modified pressure gradient, the rheodynamic lubrication equation containing inertia terms has been analyzed. Using the appropriate boundary conditions and considering externally pressurized flow in narrow clearance between two converging discs is symmetric w.r.t r and z axis, the velocity distributions, the modified pressure gradient and thereby the film pressure and the load capacity of the bearing have been obtained numerically for different values of Bingham number, Reynolds number and angle of convergence. In addition to that, the effects of the inertia forces, non-Newtonian characteristics and angle of convergence on the bearing performances have been discussed.

**Keywords**: Rheodynamic lubrication; Externally pressurized bearing; Herschel-bulkley lubricants; Angle of convergence; Load capacity.

## NOMENCLATURE

| | |
|---|---|
| $B$ | Bingham number |
| $h(r)$ | varying film thickness |
| $h_0$ | maximum film thickness |
| $p$ | pressure of the film |
| $p_a$ | atmospheric pressure |
| $Q$ | flow ratex |
| $R_1$ | radius of film inlet |
| $R_2$ | radius of film outlet |
| $r,\theta,z$ | cylindrical polar co-ordinates |
| $v_c$ | velocity of the core region |
| $v_r$ | velocity component in r directionx |
| $v_z$ | velocity component in z directionx |
| $W$ | load carrying capacity |
| $\delta(r)$ | thickness of the yield surface |
| $\dot{\gamma}$ | shear rate |
| $\eta_1$ | consistency index |
| $\eta_2$ | yield value |
| $\tau$ | deviatoric stress components |
| $\varphi$ | angle of convergence |
| $\rho$ | density of the fluid |
| $h^*,p^*,r^*,z^*$ | non-dimensional parameters of h, p, r, z |
| $\delta^*,v_c^*,v_r^*,v_z^*$ | non-dimensional parameters of $\delta(r),v_c,v_r,v_z$ |

## 1. INTRODUCTION

In the contemporary world, machinery industry immensely concentrates on the model of the bearing as well as the nature of the lubricant. To analyze the performances of the bearings adequately, it is

necessary to take into account the combined effects of fluid inertia forces and fluid viscous forces of non-Newtonian lubricants. Therefore the study of lubricant inertia is procuring increasing importance. In recent times, empirical research precisely affirms that the use of lubricants with variable viscosity can increase the property of lubrication to that of lubricants with constant viscosity. The performance of the bearing depends on the design, lubricant under consideration and many other fluid parameters.

Usage of externally pressurized thrust bearing lubricated with non-Newtonian lubricants in mechanical industries has many potential advantages. Such advantages are seen in the research works of many pioneering researchers like (El-Kayar *et. al*., 1981) and (Jaw-Ren Lin, 1999). (Amalraj *et. al*., 2013) Using externally pressurized thrust bearings lubricated with Bingham fluid Amalraj *et. al*., theoretically analyzed the effects of inertia forces. Gertzos *et. al*., has studied the Journal bearing performances and derived relative eccentricity, pressure distribution, flow rate, friction coefficient and the angle of maximum pressure (Gertzos *et. al*., 2008). Alexandros *et. al*., analyzed a creeping flow of a Bingham fluid in a lid-driven cavity and has examined the inertial effects. They also studied the strengths and weaknesses of finite volume method and the papanastasiou regulation in the lid-cavity for various Bingham and Reynolds numbers (Alexandros *et. al*., 2014). Larisa has developed an asymptotic solution for the axisymmetric squeeze flow of a viscoplastic Bingham medium by following asymptotic technique suggested earlier by Balmforth and Craster (1999) (Larisa Muravleva, 2017). Jurczak and Falicki investigated analytically the pressure distribution for the case of externally pressurized bearing and squeeze film bearing with rough surfaces lubricated with nonNewtonian fluid (Jurczak and Falicki 2016). Pavan and Vishwanath investigated the Bingham fluid between two parallel plane annuli with constant squeeze motion theoretically. Also, The effect of radius of separation on core thickness, pressure distribution, and squeeze force for various values of Bingham number is analyzed (Pavan and Vishwanath, 2017).

(Walicka *et. al*., 2017) The performance of curvulinear, externally pressurized, thrust bearing influenced by the wall porosity and roughness surfaces lubricated by non-Newtonian fluid is analyzed by Walicka *et. al*.,. Abdessamed analyzed the performance of the journal bearing are determined for various values of the non-Newtonian fluids and the numerical results computed for dilatant and pseudo-plastic fluids (Abdessamed *et. al*., 2013). (Walicka and Falicki 2015) The pressurized laminar flow of an electrorheological fluid (ERFs) of a casson type in a narrow clearance between to fixed surfaces of revolution is examined by Walicka and Falicki.

In Tribology, the effects of fluid inertia forces becomes significant. The effects of fluid inertia in lubrication have been analysed by a number of investigators. Khalil *et. al*., has investigated the effects of convective and centrifugal inertia forces, on the performance of externally pressurized conical thrust bearings, under turbulence flow condition (Khalil *et. al*., 1993). Batra and Kandasamy analyzed quantitatively the effect of inertia forces on the pressure and load carrying capacity with rheodynamic lubrication of the squeeze film bearing with circular plates (Batra and Kandasamy, 1989). Usha and Vimala discussed inertia effects in a circular squeeze film bearing containing central air bubbles (Usha and Vimala, 2000). Kandasamy and Vishwanath have studied the combined effect of fluid inertia and Bingham lubricant in a squeeze film bearing under sinusoidal squeeze motion of circular plates (Kandasamy and Vishwanath, 2007). Walicka *et. al*., investigated the inertia and couple-stress effects on the pressure distribution and load-carrying capacity in a couple stress fluid flow with the clearance of a bearing formed by two coaxial surfaces of revolution (Walicka *et. al*., 2017). Shapour and Najiafi analyzed the effect of inertial term of viscoplastic fluid flowing through a channel lined with higher compliant polymeric gel on hydroelastic stability of pressure driven flow (Shapour and Najafi, 2017). Udaya *et. al*., investigated theoretically the effect of rotational inertia and pseudoplastic in an externally pressurized flow between parallel plates and concentric spherical surfaces (Udaya *et. al*., 2011).

Many researchers have investigated inertial effect in externally pressurized thrust bearing with different types of fluids as lubricants, but very few works analyze the effects of fluid inertia forces and angle of convergence. Sinha Roy *et. al.,* observed the inertial effects in an externally pressurized thrust bearing with converging and diverging film using visco-elastic lubricant (Roy *et. al.,* 1993). Using the idea of convergence and axisymmetric in an externally pressurized converging thrust bearing the core and velovity is analyzed by (Jayakaran and Alexander, 2016).

In this research work, the effects of inertia forces on the pressure and load carrying capacity of a rheodynamic lubrication of an externally pressurized thrust bearing with an angle of convergence has been analyzed quantitatively. It has been found that the inertia effect is significant for rheodynamic lubricant in an externally pressurized converging thrust bearing. There is an appreciable increase in the bearing performance when Bingham lubricant is used. Further, it has been observed that the load capacity of the externally pressurized converging trust bearing is relatively more compared to that of the uniform externally pressurized thrust bearing with uniform plates.

## 2. MATHEMATICAL FORMULATION OF THE PROBLEM

Considering the symmetriness of the region between the circular plates of the bearing, the investigation is presented in the upper portion of the bearing. The geometry of the converging bearing is as shown in Fig.(1)

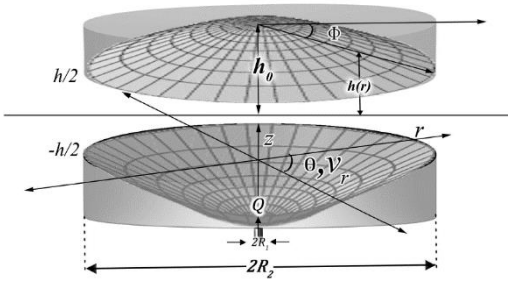


**Fig. 1. Geometry of an Externally Pressurized Convergent Thrust Bearing.**

The constitutive equation of a Bingham fluid is given by

$$\tau_{ij} = 2\left[\eta_1 + \frac{\eta_2}{I^{\frac{1}{2}}}\right] e_{ij}, \quad \left[\frac{1}{2}\tau_{ij}\tau_{ij} \geq \eta_2^2\right] \tag{1}$$

where $\tau_{ij}$ are the deviatoric stress components, $\eta_1$ and $\eta_2$ are constants namely the plastic viscosity and yield value respectively, $e_{ij}$ represents the rate of deformation components and $I = 2\ e_{ij} \times e_{ij}$ is strain invariant. However, for all practical purposes, we consider the one dimensional form of Eq. (1) which is given in Eq. (2).

$$\tau_{rz} = \eta_2 \pm \eta_1\left[\frac{\partial v_r}{\partial z}\right] \tag{2}$$

There will be a region called core region where shear stress is less than the yield stress which moves with the constant velocity, $v_c$. Let the boundaries of the core be $z = -\frac{\delta(r)h}{2}$ and $z = \frac{\delta(r)h}{2}$ as shown in Fig. (2)

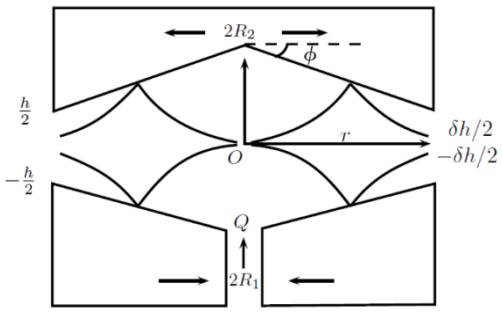


**Fig. 2. Shape of the Core in an Externally Pressurized Thrust Bearing.**

Applying basic assumptions of the lubrication theory for thin films and considering inertia forces, the governing equation can be expressed as

Equation of Continuity:

$$\frac{1}{r}\frac{\partial}{\partial r}(rv_r) + \frac{\partial v_z}{\partial z} = 0 \tag{3}$$

Equation of Momentum:

$$\rho\left[v_r\frac{\partial v_r}{\partial r} + v_z\frac{\partial v_r}{\partial z}\right] + \frac{\partial p}{\partial r} = -\frac{\partial \tau_{rz}}{\partial z} \tag{4}$$

$$\frac{\partial p}{\partial z} = 0 \tag{5}$$

The Eqs. (2) - (5) are to be solved under the following boundary conditions

$$v_r = 0 \text{ at } z = \pm\frac{h}{2} \tag{6}$$

$$v_r = v_c \text{ at } z = \pm\frac{\delta h}{2} \tag{7}$$

$$p = p_a \text{ at } r = R_2 \tag{8}$$

$$\frac{\partial v_r}{\partial z} \text{ is continuous, at } \tau = \eta_2 \tag{9}$$

## 3. SOLUTION OF THE PROBLEM

Now by the method of averaging inertia term in the Eq. (4) we get

$$\frac{\rho}{h}\left[\int_{-\frac{h}{2}}^{\frac{h}{2}}\left[v_r\frac{\partial v_r}{\partial r} + v_z\frac{\partial v_r}{\partial z}\right]dz\right] + \frac{dp}{dr} = -\frac{\partial \tau_{rz}}{\partial z} \tag{10}$$

Using continuity Eq. (3) and boundary condition (6) and (7), we get

$$\frac{2\rho}{h}\left[\frac{\partial}{\partial r}\int_0^{\frac{h}{2}} v_r^2 dz + \frac{1}{r}\int_0^{\frac{h}{2}} v_r^2 dz\right] + \frac{dp}{dr} = -\frac{\partial \tau_{rz}}{\partial z} \tag{11}$$

Now, we introduce the modified pressure gradient as

$$f = \frac{2\rho}{h}\left[\frac{\partial}{\partial r}\int_0^{\frac{h}{2}} v_r^2 dz + \frac{1}{r}\int_0^{\frac{h}{2}} v_r^2 dz\right] + \frac{dp}{dr} \tag{12}$$

By Eqs. (11) and (12), we have

$$f = -\frac{\partial \tau_{rz}}{\partial z} \tag{13}$$

Integrating Eq. (13), we get the modified pressure gradient

$\tau = -f(z) + C$ (14)Using Eq. (2) and boundary conditions (6) and (7), we get the velocity distribution in the flow region as

$$v_r = \frac{f}{2\eta_1}\left[\frac{h^2}{4}(1-\delta)^2 - \left(z - \frac{\delta h}{2}\right)^2\right], \quad \text{where} \frac{\delta h}{2} \leq z \leq \frac{h}{2} \tag{15}$$

and the velocity of the core region as

$$v_c = \frac{fh^2}{8\eta_1}(1-\delta)^2, \text{where } 0 \leq z \leq \frac{\delta h}{2} \tag{16}$$

The equation of conservation of mass for externally pressurized bearing in an integral form is given by

$$Q = 4\pi r\int_0^{\frac{h}{2}} v_r dz \tag{17}$$

Where $Q$ is the flow rate per unit width

Using velocity distributions in (17) and integrating, we obtain

$$Q = \frac{\pi r f h^3 (1-\delta)^2 (2+\delta)}{12\eta_1} \tag{18}$$

Considering the equilibrium of an element in the yield

surface $-\frac{\delta h}{2} \le z \le \frac{\delta h}{2}$, it is found that

$$f = \frac{2\eta_2}{\delta(r)h} \tag{19}$$

Hence Eq. (18) becomes

$$f = \frac{12Q\eta_1}{\pi r h^3 (1-\delta)^2 (2+\delta)} \tag{20}$$

Elimination of pressure gradient from (19) and (20), the algebric equation for determining the thickness of the yield surface $\delta(r)$ can be obtained as

$$\frac{6\eta_1 Q}{\pi r h^2 \tau_0} = \frac{(1-\delta)^2(2+\delta)}{\delta} \tag{21}$$

The variation of film thickness of the lubricant in the converging bearing can be defined as

$$h(r) = h_0 - h_0\left(\frac{r}{R_2}\right)\tan\varphi \tag{22}$$

Where, $h(r)$ represents the varying film thickness between the plates, $h_0$ is Maximum film thickness at the center of the bearing and $\varphi$ is the angle of convergence. The following non−dimensional parameters are introduced.

$$r^* = \frac{r}{R_2};\ \ \delta^* = \delta(r^*);\ \ p = \frac{p}{\frac{Q\eta_1}{\pi h_0^3}};\ \ h^* = \frac{h}{h_0};$$
$$z^* = \frac{z}{h};\ \ B = \frac{\pi R_2 h_0^2 \eta_2}{2Q\eta_1} \tag{23}$$

Here, B is the Bingham Number.

Using the non−dimensional quantities in Eqs. (15), (16) and (21), we get the velocity of the fluid in the flow region as

$$v_r^* = \frac{3}{2}\left[\frac{(1-\delta^*)^2 - (2z^*+\delta^*)^2}{r^*(1-r^*\tan\varphi)(2+\delta^*)(1-\delta^*)^2}\right], \quad \text{where } \frac{\delta^* h^*}{2} \le z^* \le \frac{h^*}{2} \tag{24}$$

Also, the velocity of the core region is

$$v_c^* = \frac{3}{2}\left[\frac{1}{r^*(1-r^*\tan\varphi)(2+\delta^*)}\right], \quad \text{where } 0 \le z^* \le \frac{\delta^* h^*}{2} \tag{25}$$

Substituting $v_r$ and $v_c$ from Eqs. (15) and (16) in to Eq. (12) and using $f$ from (18), the nondimensionalized pressure gradient will be of the form

$$\frac{dp^*}{dr^*} = \left[\frac{12}{r^*(1-r^*\tan\varphi)^3(1-\delta^*)^2(\delta^*+2)}\right] - k_1 + k_2,$$

Where

$$k_1 = Re\left[\frac{(7\delta^*+8)\tan\varphi}{(r^*)^2(1-r^*\tan\varphi)^3(\delta^*+2)^2}\right]$$

$$k_2 = Re\left[\frac{7(\delta^*)^2 + 22\delta^* + 16 + r^*(7\delta^*+2)\frac{d\delta^*}{dr^*}}{(r^*)^3(1-r^*\tan\varphi)^2(\delta^*+2)^3}\right] \tag{26}$$

Eliminating the pressure gradient from Eqs. (19) and (20), we obtain a non linear algebric equation for determining the core thickness

$$\frac{3}{Br^*(1-r^*\tan\varphi)} = \frac{(1-\delta^*)^2(2+\delta^*)}{\delta^*} \tag{27}$$

where $\delta^* = \delta r^*$ is non-dimensional core thickness for a flow Q, B is known and hence Eq. (27) can be solve. The roots of the the Eq. (27) determine the shape of the plug core region.

Differentiation (27) w.r.t $r^*$ we get

$$\frac{d\delta^*}{dr^*} = \frac{3(\delta^*)^2(3r^*\tan(\varphi)-1)}{2B\left((\delta^*)^3-1\right)(r^*)^2(1-r^*\tan(\varphi))^3} \tag{28}$$

The value of $\delta^*$ has been determined for different values of B and for various values of r*, by iterative technique and reported elsewhere (Jayakaran and Alexander, 2016). The pressure distribution can be obtained by substituting (28) in (26) and integrating using boundary condition (8) we get,

$$P^* - P_a^* = \int_{r^*}^{1}\left[\frac{dp^*}{dr^*}\right]dr^* \tag{29}$$

Where $Re = \frac{3\rho Q h_0}{20\pi\eta_1 R_2^2}$ is the Reynolds number. The pres

sure distribution has been calculated for different values of Bingham number, Reynolds number and Angle of convergence numerically. Again, the load carrying capacity W for the externally pressurized thrust bearing can be obtained by integrating the pressure over the entire region and we get

$$W = \int_{R^*}^{1}\left(P^* - P_a^*\right) r^* dr^* \tag{30}$$

where, $R^* = \frac{R_1}{R_2}$ is the ratio of inside to outside radius of the bearing. This integration is performed

numerically for various values of the *Re*, *B*, and φ.

## 4. RESULTS AND DISCUSSION

The radial distribution of the film pressure has been obtained for various values of Bingham number (B), Reynolds number (Re) and the Angle of convergence (φ) are shown in Figs. (3), (4) and (5). The pressure is maximum in orifice and gradually decreases to the Periphery. We observe that the pressure tends to increase with the increase in Bingham number, Reynolds number and Angle of convergence. However, the quantum of increase is less for high Reynolds number. Moreover, increase in pressure is more significant when angle of convergence is increased.

The Numerically computed results of load carrying capacity for various Bingham number, Reynolds number and Angle of convergence for different levels of inlet radius are given in the tables (1)-(4). It is observed from the analysis that there is an appreciable increase in the value of the load capacity for the Bingham lubricants relative to that of Newtonian lubricant. This is due to the fact that Bingham, being a thick viscous model, shows a high load carrying capacity. Further, the load carrying capacity of the bearing has been found to increase gradually with the increase of Reynolds number. However, the quantum of increase is less for high Reynolds number as shown in Figs. (6) and (7).

The angle of convergence helps to increase the load capacity of the bearing when we increase it, up to a particular position, as shown in Figs. (8) and (9). Beyond this critical angle ($\varphi < 30^{\circ}$) the load carrying capacity of the bearing starts to deteriorate with increase in Reynolds number for any B and R* as shown in Fig. (10). When the inlet radius R* decreases we expect the increasing trend in the workload as it's observed and shown in the Fig. (11).

The inertia plays a small role in the bearing performance. For B = 5 & B = 10 , φ = 0 to φ = 25 and R*=0.05 & R*=0.1 the change in percentage of increase in the load capacity due to inertia forces are shown in tables (4)-(6). From the results it is observed that the percentage increase in load capacity reduces for materials with larger yield value and increases in angle of convergence. Further, this percentage increase is found to increase with an increase in Reynolds Number but percentage decreases as the angle of convergence increases for any Bingham Number. Even though the load carrying capacity of the bearing is found to increase with an increase of Reynolds number, the increase is not much for high viscous fluids i.e for fluids with high Bingham Number. For a the particular angle of convergence (φ = 0) which corresponds to flat externally pressurized thrust bearing, our results are found to be matching with results of (Jayakaran *et. al*., 2010).

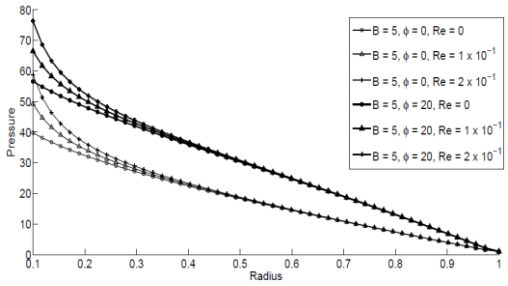


**Fig. 3. Pressure profile for various Reynolds Number and Angle of Convergence for B =5.**

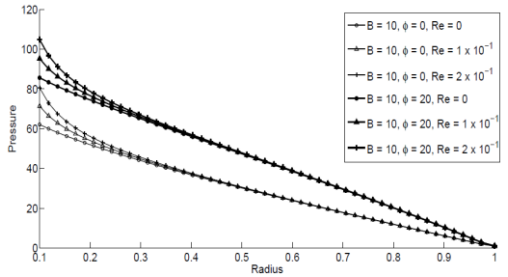


**Fig. 4. Pressure profile for various Reynolds Number and Angle of Convergence for B =10.**

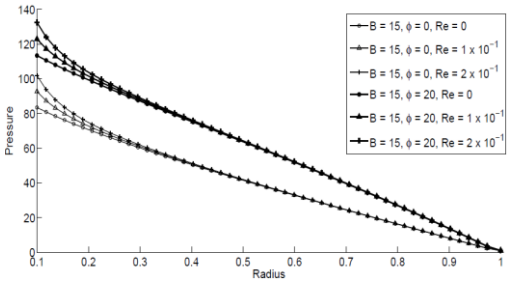


**Fig. 5. Pressure profile for various Reynolds Number and Angle of Convergence for B = 15.**

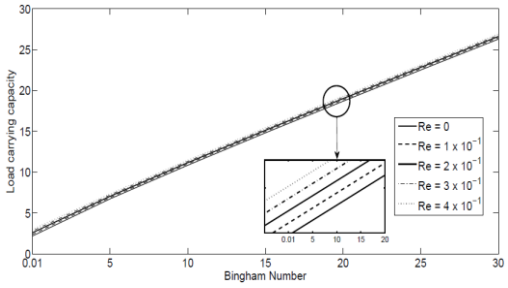


**Fig. 6. Load carrying capacity for various Reynolds Number & Bingham Number for φ=5.**

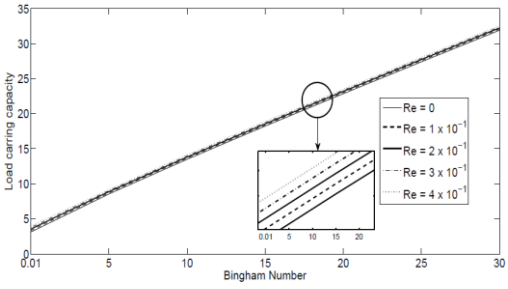


**Fig. 7. Load carrying capacity for various Reynolds Number & Bingham Number for φ = 15.**

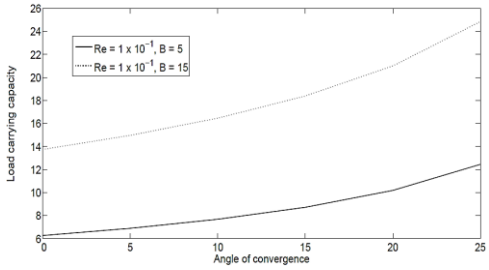


**Fig. 8. Load carrying capacity for various Angle of Convergence.**

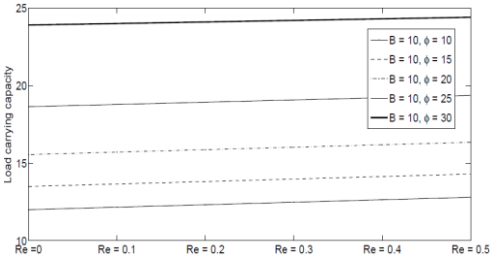


**Fig. 9. Load carrying capacity for various Reynolds Number and $\varphi \leq 30^{\circ}$ for B = 5 with Inlet Radius $R^{*}$ = 0.1.**

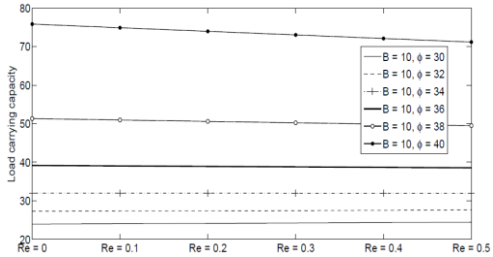


**Fig. 10. Load carrying capacity for various Reynolds Number and $\varphi > 30^{\circ}$ for B = 5 with Inlet Radius $R^{*}$ = 0.1.**

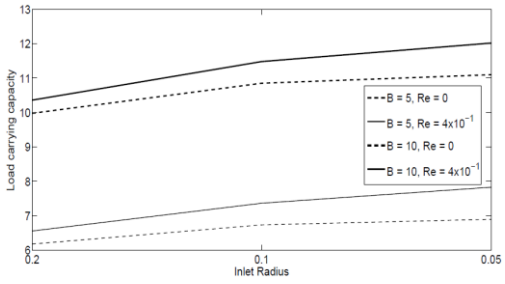


**Fig. 11. Load carrying capacity for various Reynolds Number, Bingham Number and Inlet Radius for $\varphi$ = 5.**

**Table 1 Load Capacity for different value of Re and Angle of Convergence for B = 5 and $R^{*}$ = 0.05**

| B=5 | Reynolds number ($\times 10^{-1}$) | | | | |
|---|---|---|---|---|---|
| | 0 | 1 | 2 | 3 | 4 |
| φ=0 | 6.26 | 6.50 | 6.72 | 6.95 | 7.18 |
| φ=5 | 6.89 | 7.13 | 7.36 | 7.60 | 7.83 |
| φ=10 | 7.69 | 7.93 | 8.16 | 8.40 | 8.63 |
| φ=15 | 8.74 | 8.99 | 9.22 | 9.46 | 9.67 |
| φ=20 | 10.23 | 10.47 | 10.70 | 10.94 | 11.17 |
| φ=25 | 12.53 | 12.75 | 12.97 | 13.2 | 13.42 |

**Table 2 Load Capacity for different value of Re and Angle of Convergence for B = 5 and $R^{*}$ = 0.1**

| B=5 | Reynolds number ($\times 10^{-1}$) | | | | |
|---|---|---|---|---|---|
| | 0 | 1 | 2 | 3 | 4 |
| φ=0 | 6.12 | 6.27 | 6.42 | 6.57 | 6.73 |
| φ=5 | 6.73 | 6.89 | 7.05 | 7.20 | 7.36 |
| φ=10 | 7.51 | 7.68 | 7.84 | 7.99 | 8.16 |
| φ=15 | 8.56 | 8.72 | 8.88 | 9.04 | 9.20 |
| φ=20 | 10.03 | 10.18 | 10.34 | 10.50 | 10.66 |
| φ=25 | 12.30 | 12.44 | 12.59 | 12.73 | 12.88 |

**Table 3 Load Capacity for different value of Re and Angle of Convergence for B=10 and R=0.1**

| B=10 | Reynolds number ($\times 10^{-1}$) | | | | |
|---|---|---|---|---|---|
| | 0 | 1 | 2 | 3 | 4 |
| φ=0 | 9.92 | 10.07 | 10.23 | 10.38 | 10.53 |
| φ=5 | 10.85 | 11.01 | 11.16 | 11.32 | 11.47 |
| φ=10 | 11.99 | 12.16 | 12.32 | 12.47 | 12.64 |
| φ=15 | 13.49 | 13.65 | 13.81 | 13.97 | 14.13 |
| φ=20 | 15.55 | 15.71 | 15.87 | 16.02 | 16.18 |
| φ=25 | 18.64 | 18.78 | 18.93 | 19.07 | 19.22 |

**Table 4 Change in Percentage in load Capacity with respect to Re=0 for B = 5 when $R^{*}$ = 0.05**

| B=5 | Reynolds number ($\times 10^{-1}$) | | | | |
|---|---|---|---|---|---|
| | 1 | 2 | 3 | 4 | 5 |
| φ=0 | 3.51 | 6.80 | 9.85 | 12.72 | 15.4 |
| φ=5 | 3.27 | 6.33 | 9.20 | 11.90 | 14.45 |
| φ=10 | 2.98 | 5.80 | 8.44 | 10.95 | 13.33 |
| φ=15 | 2.65 | 5.16 | 7.55 | 9.82 | 11.99 |
| φ=20 | 2.25 | 4.40 | 6.45 | 8.42 | 10.31 |
| φ=25 | 1.74 | 3.42 | 5.04 | 6.61 | 8.12 |

**Table 5 Change in Percentage in load Capacity with respect to Re=0 for B = 5 when $R^{*}$ = 0.1**

| B=5 | Reynolds number ($\times 10^{-1}$) | | | | |
|---|---|---|---|---|---|
| | 1 | 2 | 3 | 4 | 5 |
| φ=0 | 2.44 | 4.77 | 6.98 | 9.10 | 11.13 |
| φ=5 | 2.28 | 4.46 | 6.54 | 8.53 | 10.44 |
| φ=10 | 2.08 | 4.08 | 6.01 | 7.85 | 9.62 |
| φ=15 | 1.85 | 3.63 | 5.34 | 7.00 | 8.6 |
| φ=20 | 1.55 | 3.05 | 4.50 | 5.91 | 7.29 |
| φ=25 | 1.15 | 2.28 | 3.38 | 4.45 | 5.51 |

**Table 6 Change in Percentage in load Capacity with respect to Re=0 for B = 10 when $R^{*}$ = 0.1**

| B=10 | Reynolds number ($\times 10^{-1}$) | | | | |
|---|---|---|---|---|---|
| | 1 | 2 | 3 | 4 | 5 |
| φ=0 | 1.52 | 2.99 | 4.42 | 5.80 | 7.15 |
| φ=5 | 1.43 | 2.81 | 4.16 | 5.50 | 6.75 |
| φ=10 | 1.32 | 2.60 | 3.85 | 5.07 | 6.25 |
| φ=15 | 1.19 | 2.33 | 3.46 | 4.56 | 5.64 |
| φ=20 | 1.01 | 1.99 | 2.96 | 3.91 | 4.84 |
| φ=25 | 0.77 | 1.52 | 2.27 | 3.00 | 3.72 |

## 5. CONCLUSION

The above investigations reveals that the increase in Bingham number, Reynolds number and the Angle of convergence significantly enhances the bearing performance such as pressure distribution and load carrying capacity. However the effect of fluid inertia on the bearing performance is found to be significant when the inlet is small.

## ACKNOWLEDGMENTS

The authors thank the Principal and management of SSN institutions for their support in carrying out this work.

## REFERENCES

Abdessamed N., S. Larbi, H. Belhaneche, and M. Malki (2013). Journal Bearings Lubrication Aspect Analysis Using Non-Newtonian Fluids. *Advances in Tribology*, 1-9.

Alexandros S., G. C. Georgiou and A. N. Alexandrou (2014). Performance of the finite volume method in solving regularised Bingham flows: Inertia effects in the lid-driven cavity flow. *Journal of Non-Newtonian Fluid Mechanics*, 208-209, 88-107.

Amalraj, I. J., S. Narasimman and A. Kandasamy (2013). Inertia Effects in Rheodynamic Lubrication of an Externally Pressurized Thrust Bearing Using Bingham Lubricant with Sinusoidal Injection. *Journal of Applied Fluid Mechanics* 6(4), 609-616.

Balmforth, N. J. and R. V. Craster (1999). Ocean waves and ice sheets, *J. Fluid Mech*. 395, 89-124

Batra, R. L. and A. Kandasamy (1989). Inertia effects in rheodynamic lubrication of a squeeze film bearing. Wear, Elsevier Sequoia S. A., (in Netherlands), 273-282.

El-Kayar, A., E. A. Salem and M. F. Kalil (1981). Behaviour of Externally Pressurized Conical Bearings Lubricated With non-Newtonian Fluids. Wear, Elsevier Sequoia S.A., Lausanne (in Netherlands), 133-145.

Gertzos, K. P., P. G. Nikolakopoulos and C. A. Papadopoulos (2008). CFD analysis of journal bearing hydrodynamic lubrication by Bingham lubricant. *Tribology International* 41, 1190-1204.

Jafargholinejad S. and M. Najafi. (2017). Inertia flows of Bingham fluids through a planar channel: Hydroelastic instability analysis. *Journal of Mechanical Engineering Science* 232(13), 2394-2403.

Jaw-Ren L. (1999). Static and dynamic characteristics of externally pressurized circular step thrust bearings lubricated with couple stress fluids. *Tribology International* 32, 207-216.

Jayakaran Amalraj, I. and G. Alexander Raymand (2016). Core Variation in an Externally Pressurized Converging Thrust Bearing with Bingham Lubricant. *Applied Mechanics and Materials* 852, 428-428.

Jayakaran A., I., S. Narasimman and A. Kandasamy (2010). Inertia Effects in Rheodynamic Lubrication of an Externally Pressurized Thrust Bearing using Bingham Fluids. *8th Asian Computational Fluid Dymanics Conference*, Hong Kong SAR, (in China).

Jurczak, P. and J. Falicki (2016). Pressure Distribution in a Squeeze Film Spherical Bearing with Rough Surfaces Lubricated by an Ellis Fluid. *Int. J. of Applied Mechanics and Engineering* 21(3), 593-610.

Kandasamy, A. and K. P. Vishwanath (2007). Rheodynamic Lubrication of a squeeze film bearing under sinusoidal squeeze motion. *Computational and Applied mathematics*, 26, 381-396.

Khalil, M. F., S. Z. Kassab and A. S. Ismail (1993). Effect of inertia forces on the performance of externally pressurized conical thrust bearing under turbulent flow condition. *Wear* 166(2), 155-161.

Larisa M. (2017). Axisymmetric squeeze flow of a viscoplastic Bingham medium. *Journal of Non-Newtonian Fluid Mechanics* 249, 97-120.

Singeetham P. K. and K. P. Vishwanath (2017). Squeezing of Bingham Fluid Between Two Plane Annuli. *Applications of Fluid Dynamics, Lecture Notes in Mechanical Engineering*, 385-396.

Sinha Roy, J., S. Padhy and L. K. Bhopa (1993). Inertia effect in externally pressurized thrust bearing with converging and diverging film using visco-elastic lubricant. *Actamechanica, Springer-Verlag* 96, 1-12.

Udaya, P. S., R. S. Gupta and V. K. Kapur (2011). Effects Of Inertia In The Steady State Pressurised Flow Of A Non-Newtonian Fluid Between Two Curvilinear Surfaces Of Revolution: Rabinowitsch Fluid Model. *Chemical and Process Engineering* 32(4), 333-349.

Usha, R. and P. Vimala (2000). Inertia effects in circular squeeze film containing a central air bubble. *Fluid Dynamics Research* 26, 149-155.

Walicka, A. and J. Falicki (2015). Reynolds number effects in the flow of an electrorheological fluid of a Casson type between fixed surfaces of revolution. *Applied Mathematics and Computation* 250, 636-649.

Walicka, A., E. Walicki, P. Jurczak and J. Falicki

(2017). Influence of Wall Porosity and Surfaces Roughness on the Steady Performance of an Externally Pressurized Hydrostatic Conical Bearing Lubricated by Rabinowitsch Fluid. *J. of Applied Mechanics and Engineering* 22(3), 717-737.

Walicka, A., P. Jurczak and J. Falicki (2017). Inertia and Couple-Stress Effects in a Curvilinear Thrust Hydrostatic Bearing. *J. of Applied Mechanics and Engineering* 22(2), 759-767.